Noise Characteristics of Semiconductor Laser with Phase-Conjugate Feedback

M.I. Azawe
Department of Physics,
College of Education, Mosul University

Received 23/2/2005 **Accepted** 24/10/2005

الخلاصة

أطياف الضوضاء الناتجة من تعرض ليزر أشباه الموصلات الى تغذية مرتدة ذات الطور المرافق قد تم بحثها نظرياً. معادلات المعدل للزمن المتواني مع التغذية المرتدة فد تم حلها لأجل إشتقاق المعادلات المخصصة لأطياف ضوضاء الشدة النسبية و ضوضاء التردد. النتائج العددية أظهرت أن ذروة الأسترخاء الرنيني قد تحركت الى موضع ترددي أخر تحدده كمية التغذية المرتدة. و تعتبر هذه من الناحية التقنية مهمة لأجل تحسين عرض نطاقها الترددي. مستوي الضوضاء تأثر بمعلمات التغذية المرتدة، و هي زمن الأستجابة و معدل التغذية.

ABSTRACT

Noise spectra of semiconductor laser subject to a phase-conjugate feedback were investigated theoretically. Time-delayed rate equations with feedback were solved and characteristic equations for relative intensity noise and frequency noise spectra were derived. Numerical results indicate that the relaxation resonance peak was moved to a new frequency region determined by the amount of feedback. This is a technological importance for the improvement of modulation bandwidth. Noise level was affected by the feedback parameters, mainly; the response time and the feedback rate.

I.INTRODUCTION

Semiconductor lasers (SLs) are very attractive sources for optical communication and optical read-out systems [1]. On the other hand, highly coherent laser sources with wide continuous frequency tuning range are also required in many spectroscopic applications [2]. The usefulness of SL in coherent optical systems that require low phase noise is hampered by their large linewidth [3] and sensitivity to external optical feedback [4]. Optical feedback (OF) from a phase-conjugate mirror (PCM) is preferred over conventional optical feedback [5]. In the later case, the SL suffers from extreme sensitivity to mirror-distance variations within an optical wavelength [6]. For phase-conjugate feedback (PCF) one is always confronted with a certain sluggishness of the reflector owing to the finite response time which should be taken into account when analyzing the SL stability [7]. For stabilization purpose, the laser with PCF having the phase as an independent on the mirror position [8], allows the linewidth to be decreased [9]. Recent data on the linewidth of free-running quantum cascade lasers (~150 kHz) was reported [10], and more reduction in the linewidth can be provided with PCF.

The analysis of nonlinear rate equations for the determination of the noise spectra of SL subjected to OF from phase-conjugate mirror will be presented in this paper. The analysis will be based on single mode operation of the SL with PCF taking into account the:

1-the finite response time effect in the PCM

2-nonlinaer gain coefficient

3-spontaneous emission rate coupled to the lasing mode.

The plane of the paper is as follows. Section II describes the single mode rate equations and the evaluation of the time evolution of small perturbations from the steady-state of the SL operation. Section III will be devoted to the noise spectra by Fourier transform from the linearized rate equations containing the Langevin noise terms. The applied technique will be used for calculating the results in Section IV. Conclusions of the main results will be presented in Section V. Mathematical details are described in the Appendix.

II. RARE EQUATIONS

The rate equations for single mode SL with PCF are given by [3, 9]:

$$E^{\bullet}(t) = \frac{1}{2}(1+i\alpha)\Gamma G_N (N - N_{th})E(t) + \frac{\gamma_{PCM}}{t_m}\exp\left[-2i\delta\left\{t-\frac{\tau}{2}\right\}\right]\exp(i\Phi_{PCM})E^{*}(t-\tau) \quad (1)$$

$$N^{\bullet}(t) = J(t) - \frac{N(t)}{\tau_{sp}} - G_N (N - N_{th})\{1-\varepsilon P(t)\}P(t) \quad (2)$$

Where $N(t)$ is the number of electron-hole pairs (inversion) in the active region, and

$\tau = \frac{2L}{c}$ is the external roundtrip time;

τ_{sp} the carrier lifetime;

Γ confinement factor;

δ detuning of external mirror;

G_N differential gain;

N_{th} is the number of carriers at threshold of the solitary laser diode;

$E(t)$ is the slowly varying amplitude of the optical field;

α linewidth enhancement factor;

$J(t)$ number of carriers injected into the active region per unit time;

$P(t)$ number of photons inside the laser diode cavity with $P(t) = |E(t)|^2$;

Φ_{PCM} phase due to PCM;

t_m response time of the mirror;

ε nonlinear gain parameter;

γ_{PCM} feedback rate due to phase-conjugate mirror.

The feedback term in (1) depends on the optical field at and before time $t-\tau$ [3]. If the scaling time **Ω** taken with the laser relaxation oscillations (RO) frequency ω_R , useful approximations of the stability boundaries can be derived for small **Ω** [10].

The injection field from the PCM can be written as [3]:

$$E_{PCM}(t)=\frac{1}{t_m}\exp\left[2i\delta\left(t-\frac{\tau}{s}\right)\right]\int_{-\infty}^{t}E^{*}(t-\tau)\exp\left[-\left(\frac{1}{t_m}+i\delta\right)(t-\theta)\right]d\theta \qquad (3)$$

where θ is any time before feedback. The rate equation in (1) can be split into two equations, and taking into consideration the initial condition satisfying (3). The following equation relates the optical field and the number of photons:

$$E(t)=\sqrt{P(t)}\exp[i\Phi(t)] \qquad (4)$$

$$E_{PCM}(t)=\sqrt{P_{PCM}(t)}\exp[i\Phi_{PCM}(t)] \qquad (5)$$

where $\Phi(t)$ is the phase without feedback.

The above equations will be used for obtaining $P,\Phi,\Phi_{PCM},P_{PCM}$, and N, from the numerical integration of the followings:

$$P^{\bullet}(t)=\Gamma G_N\Delta NP(t)+2\gamma_{PCM}\sqrt{P(t)P_{PCM}(t)}\cos[\Phi(t)-\Phi_{PCM}(t)] \qquad (6)$$

$$\Phi^{\bullet}(t)=\frac{1}{2}\Gamma\alpha\Delta NG_N-\gamma_{PCM}\sqrt{\frac{P_{PCM}(t)}{P(t)}}\sin[\Phi(t)-\Phi_{PCM}(t)] \qquad (7)$$

$$P^{\bullet}_{PCM}(t)=-\frac{2}{t_m}P_{PCM}(t)+\frac{2}{t_m}\sqrt{P(t-\tau)P_{PCM}(t)}\cos[\Phi(t-\tau)+\Phi_{PCM}(t)-2\delta(t-\tau/2)] \qquad (8)$$

$$\Phi^{\bullet}_{PCM}(t)=\delta-\frac{1}{t_m}\sqrt{\frac{P(t-\tau)}{P_{PCM}(t)}}\sin[\Phi(t-\tau)+\Phi_{PCM}(t)-2\delta(t-\tau/2)] \qquad (9)$$

$$N^{\bullet}(t)=J(t)-\frac{N(t)}{\tau_{sp}}-G_N\Delta N(1-\varepsilon P(t))P(t) \qquad (10)$$

where $\Delta N=N(t)-N_{th}$, the number of electron-hole pairs (inversion) in the active region. The Langevin noise terms had been disregarded provide that the emission of the laser diode assumed to be single frequency and constant light output. This state can be reached when the laser diode was locked to the frequency δ of the mirror pump-beams as:

$$\Phi(t)=\delta.t+\Phi_S \qquad (11)$$

$$\Phi_{PCM}(t)=\delta.t-\Phi_S \qquad (12)$$

where Φ_S is at steady-state operation of the laser diode.

Steady-state operation of the SL can be reached when the deviations decay and allow the rate equations to be linearized. Defining $\chi(t)$ as a deviation from the steady-state then:

$$\chi(t)=\left(P(t)-P_S,\Phi(t)-\delta.t-\Phi_S,N(t)-N_S,P_{PCM}(t)-P_S,-\Phi_{PCM}+\delta.t-\Phi_S\right) \qquad (13)$$

where P_S,Φ_S,N_S are the steady-state values.

Assuming a solution of an exponential time-dependence for the above equations as:

$$\chi(t) \rightarrow \exp(\gamma.t) \tag{14}$$

and for delay-differential equations as:

$$\chi(t-\tau) \rightarrow \chi(t)\exp(-\gamma.t) \tag{15}$$

$$\chi(t-\tau) \rightarrow \exp(\gamma.t)\exp(-\gamma.\tau) \tag{16}$$

The rate equations can now be written with the addition of Langevin noise terms as:

$$\chi^{\bullet}(t) = A\chi(t) + A^{'}\chi(t-\tau) + F(t) \tag{17}$$

where $F(t)$ is the Langevin noise term.

The system can be formally solved using Laplace-transform techniques [1]:

$$(\gamma.I - A - \exp(-\gamma.\tau))\tilde{\chi}(\gamma) = \chi(0) \tag{18}$$

where I is the unit matrix. The system can be regarded as stable, if and if all the roots of the characteristics equation:

$$D(\gamma) = \det(\gamma.I - A - A\exp(\gamma.\tau)) \tag{19}$$

is equal to zero.

Writing the full γ-dependence of $D(\gamma)$ yields:

$$D(\gamma) = \gamma^5 + d_4\gamma^4 + d_3\gamma^3 + \{d_{20} + d_{21}\exp(-\gamma.\tau)\}\gamma^2 + \{d_{10} + d_{11}\exp(-\gamma.\tau) + d_{12}\exp(-2\gamma.\tau)\}\gamma$$
$$+ \{d_{00} + d_{01}\exp(-\gamma.\tau) + d_{02}\exp(-2\gamma.\tau)\} \tag{20}$$

where the coefficients d_i are functions of the laser parameter under steady-state conditions [see Appendix A for the coefficients of d_i].

III. NOISE SPECTRA

To obtain the optical spectra of the laser system, Fourier transformation had to be performed in the form:

$$\tilde{\chi}(\omega) = (i\omega.I - A - A^{-1}\exp(-i\omega.\tau))^{-1}\tilde{F}(\omega) \tag{21}$$

where $\tilde{\chi}(\omega)$ is the Fourier transform of $\chi(t)$, and $\tilde{F}(\omega)$ is also the Fourier transform of the Langevin noise $F(t)$. The power and the phase are of the form [1]:

$$\delta.\tilde{P}(\omega) = \frac{1}{\Delta(\omega)}\left[M_{11}(i\omega)\tilde{F}_P(\omega) - M_{21}(i\omega)\tilde{F}_{\Phi}(\omega)\right] \tag{22}$$

$$\delta.\tilde{\Phi}(\omega) = \frac{1}{\Delta(\omega)}\left[-M_{12}(i\omega)\tilde{F}_P(\omega) + M_{22}(i\omega)\tilde{F}_{\Phi}(\omega)\right] \tag{23}$$

with $\Delta(\omega)$ is the determinant of $\{i.\omega.I - A - A'\exp(-i\omega.\tau)\}$. $D(\gamma)$ can be found by Laplace transformation and $\Delta(\omega)$ is equal to $D(i\omega)$. $M_q(i\omega)$ are the minors of $\{i.\omega.I - A - A'\exp(-i\omega.\tau)\}$. [See the Appendix B for $M_q(i\omega)$] The relative intensity noise (RIN) and the frequency noise spectrum (FNS) are:

$$S_{RIN}(\omega) = \frac{R}{|\Delta|^2\sqrt{2\pi}}\left[|M_{11}|^2\frac{2}{P_S} + |M_{12}|^2\frac{1}{2P_S^3}\right] \tag{24}$$

$$S_{\Phi}(\omega) = \frac{\omega^2}{|\Delta|^2 \sqrt{2\pi}} \left[|M_{21}|^2 2RP_S + |M_{22}|^2 \frac{R}{2P_S} \right] \quad (25)$$

where R is the rate of spontaneous emission, and is given by $R = 4\beta.N$. β is the fraction of this emission coupled into the lasing mode.

IV. RESULTS

A. Relative Intensity Noise (RIN)

In order to decrease the influence of spontaneous emission in the intensity fluctuations, the laser will be assumed to be pumped around more than at least 5% above threshold (gain will be more than losses). The laser parameters that have been used in the numerical simulations are listed in Table 1 below. The angular RO frequency of the solitary laser can be found the relation $\omega_R = \sqrt{\frac{G_N P_o}{\tau_p}}$, with P_o is the number of photons at the inversion above threshold. τ_p is the photon lifetime. The stable region of laser operation with OF will be considered and investigated for low-feedback ($\gamma_{PCM} \leq 100 \times 10^7\ \text{sec}^{-1}$) and then for high-feedback ($\gamma_{PCM} \leq 1500 \times 10^7\ \text{sec}^{-1}$) regimes. Eriksson had related the nonlinear regions of laser diode dynamics to the RO frequency relative to free-running laser diode [11].

Fig.(1) represents the numerical results of Eq.(24), the RIN for the laser diode with PCF and for two different values of the response time t_m of 100 psec and 400 psec in the low-feedback regime. Notice that, a resonance peak has occurred when the applied frequency was equal to the RO frequency at that power. There is a substantial rise in the RO peak when the response time t_m was increased. Erneux et al. considered a beating phenomenon between the RO peak and the regimes of exhibiting frequencies close to external cavity frequency [12].

The influence of increasing the number of photons (power output) on the RIN spectra was conducted in order to see its effect, as in Fig.(2). A distinct effect of the photon on the RIN spectra is clear from the figure. When the pumping current was increased from $1.04J_{th}$ to $1.06J_{th}$, which means the increase of power output, the resonance peak was shifted to a higher value. This is due to the increase of RO frequency with the power output as mentioned before. Also, it can be noticed that there is a decrease in the RIN value with the increase of pumping.

Fig.(3) illustrates the effect of the delay time τ in the external cavity on the RIN spectra at the low-feedback operation of the laser diode (stable operation). The height of the RO peak changes with τ, predicting that when $\omega_R \tau = p.2\pi$, where p is an integer, a strong coupling between the two cavities will exist giving rise to an enhancement in the RO peak. If $\frac{\omega_R.\tau}{2\pi}$ is not an integer, then due to phase mismatch, no coupling will exist.

RIN spectra of the laser in two different feedback levels were studied and the results are shown in Fig.(4). The strength of OF had a clear effect on the RO resonance peak. This resonance is attributed to the inversion dependence of the intrinsic laser resonance, where the inversion is changed due to feedback as a result of reflected photons back to the laser cavity from the external mirror. Furthermore, the overall noise level was decreased due to the increase of the level of feedback.

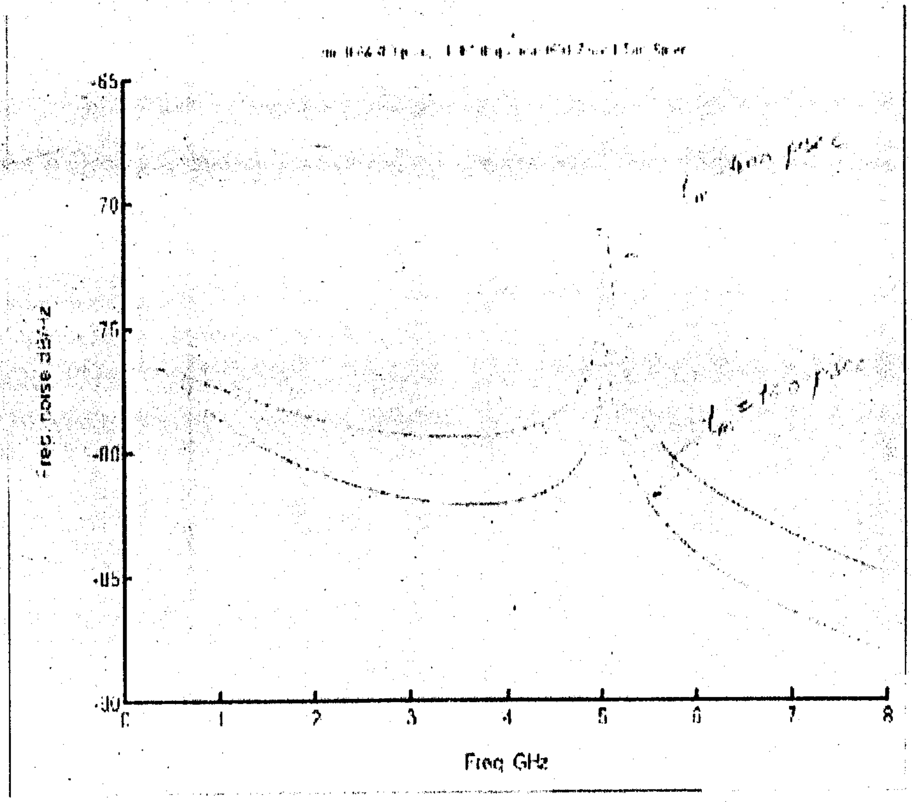

Fig.(1):Shows the RIN spectra of the laser diode with PCF for two different values of response time t_{m}, 100 psec and 400 psec.

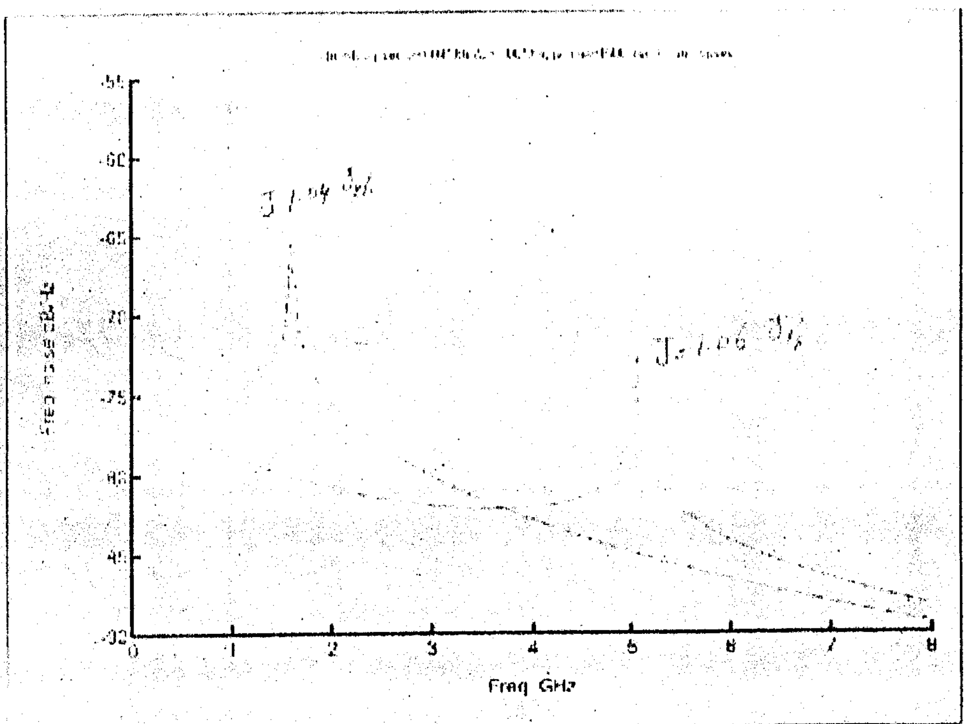

Fig.(2):Illustrates the influence of pumping (increase of photons) on the RIN spectra. Inversion values were J=1.04 J_{th} and J=1.06 J_{th}. Two resonance peaks are shown for the RO frequency.

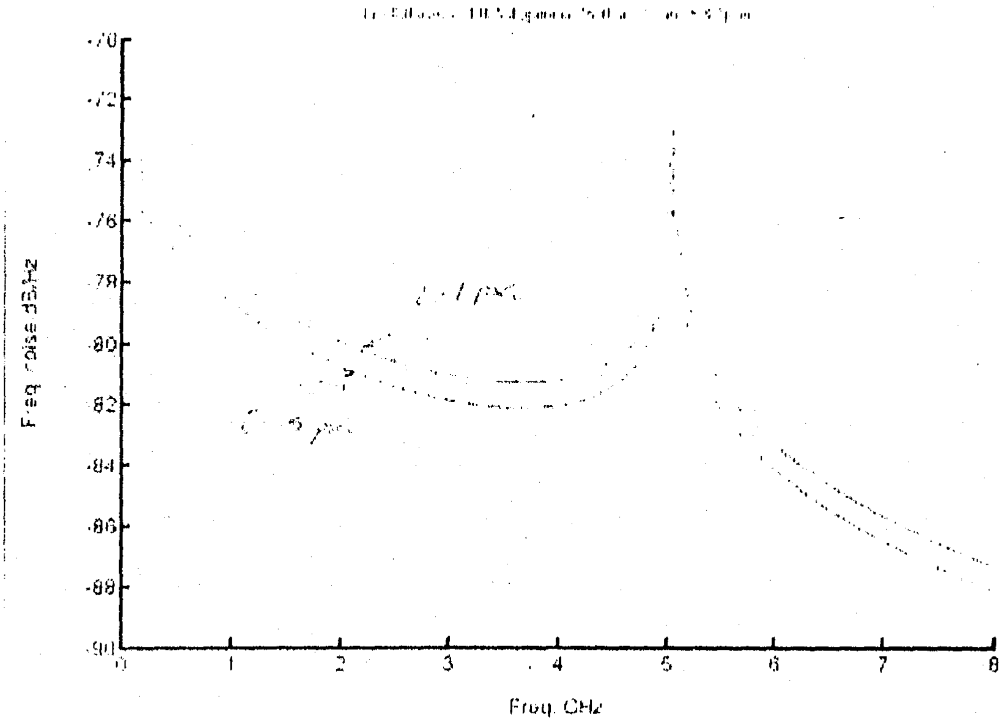

Fig.(3):Represents the effect of time delay in the external cavity on the RIN spectra. Inversion value was J=1.06 J_{th}.

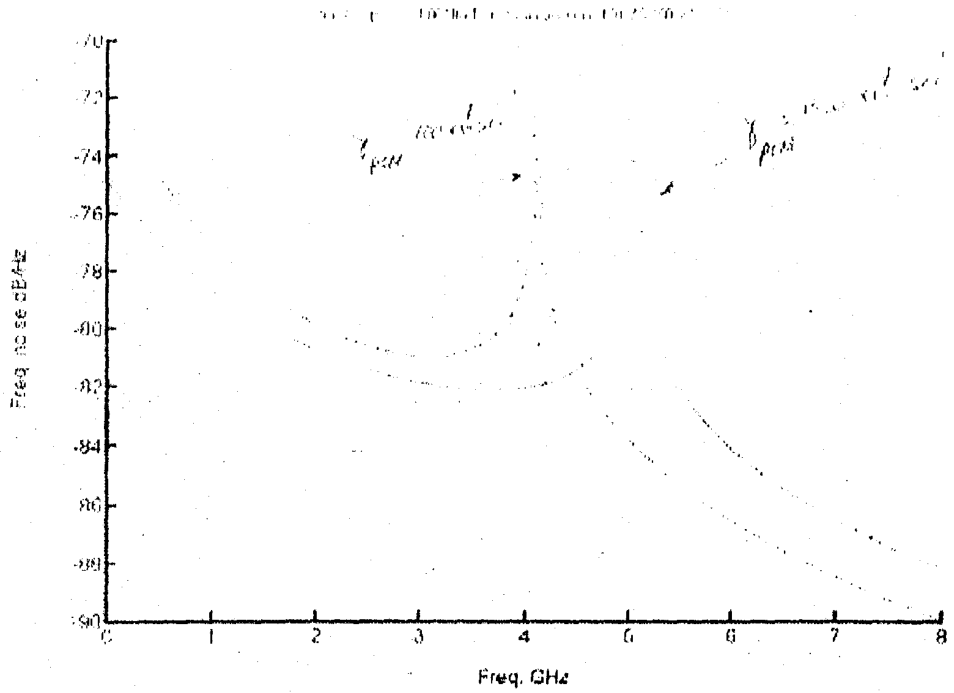

Fig.(4):Represents the effects of γ_{PCM} feedback rate due to phase-conjugate mirror on the RIN spectra. Inversion value was J=1.06 J_{th}.

9

B. Frequency Noise Spectra (FNS)

We observed from the simulation of the relative intensity noise (RIN), that a strong resonance peak around the RO frequency had occurred. In case of frequency noise spectrum (FNS), especially when the nonlinear gain parameter (ε=0), a suppression of the relaxation peak was found, predicting a strong damping in the system. This feature can be seen in Fig.(5). But the inclusion of gain nonlinearity in the numerical simulation had produced a pronounced resonance peak around the RO frequency. The disappearance of resonance peak when the laser diode was modulated in the frequency region around the RO for linear gain, suggests that the gain can play a great role in the modulation characteristics. Linear gain in the laser operation means low power output.

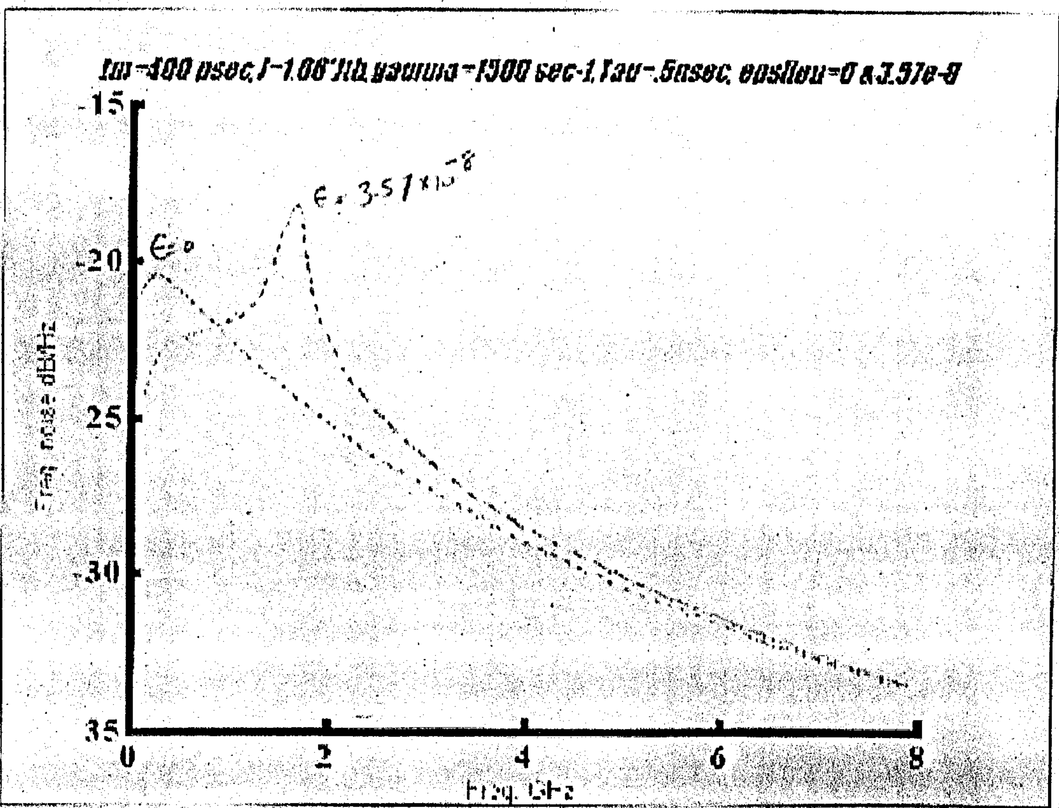

Fig.(5):Shows the effects of nonlinear gain coefficient on the FNS spectra of the laser diode, for high-feedback rate 1500e7 sec-1.

Fig.(6) represents the effects of γ_{PCM} on the FNS of the laser for two values of feedback, the low-feedback and the high-feedback. In addition to the shift of the resonance peak due to the increase of γ_{PCM} as a result of the feedback on the inversion, it has an overall effect on the spectra.

The characteristics of FNS spectra due to other parameters; the mirror response time t_m, time delay in the external cavity τ, and the injection were also studied, similar to the RIN spectra.

To summarize the influence of pumping (inversion) and the feedback rate on the noise characteristics of the semiconductor laser, a 3-D plots were used for the simulation to illustrate these effects. Fig.(7) and Fig.(8) indicate how the resonance peak was shifted towards higher frequency when both the pumping and γ_{PCM} were increased. RIN spectra were shown in bold and FNS in flint lines.

The spectra agree in some aspects with those obtained by van der Graaf et al [3]. There is one clear discrepancy: they did not observe a shift of the RO frequency with the applied frequency in the laser output operating with PCF. This is due to the fact they assumed a linear gain (ε 0) in their simulation. Noise spectra; RIN and FNS, were all approached zero when ω→0. This is because of the phase compensating nature of the PCM which fixes the phase in the long run.

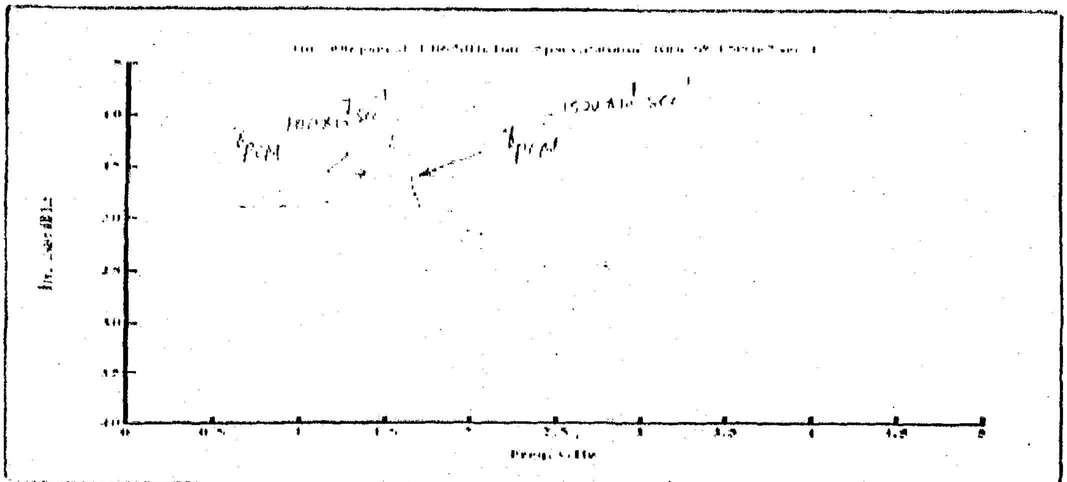

Fig.(6):Shows the effects of γ_{PCM}, feedback rate due to phase-conjugate mirror on the FNS spectra, with response time is 400 μsec.

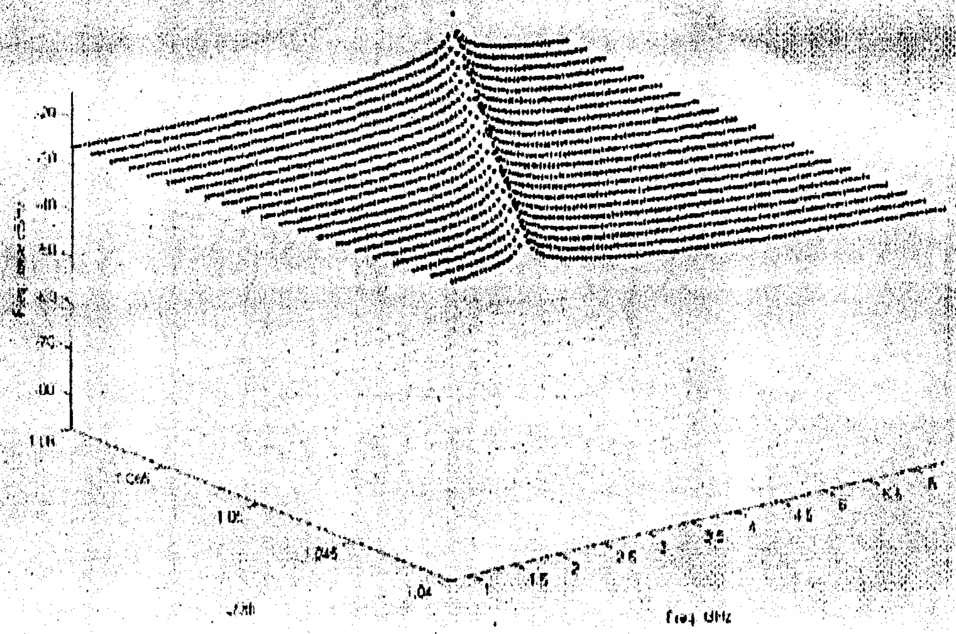

Fig.(7):Noise spectra of the laser diode as a function of normalized injection and frequency. Response time was 400 psec and with the inclusion of nonlinear gain.

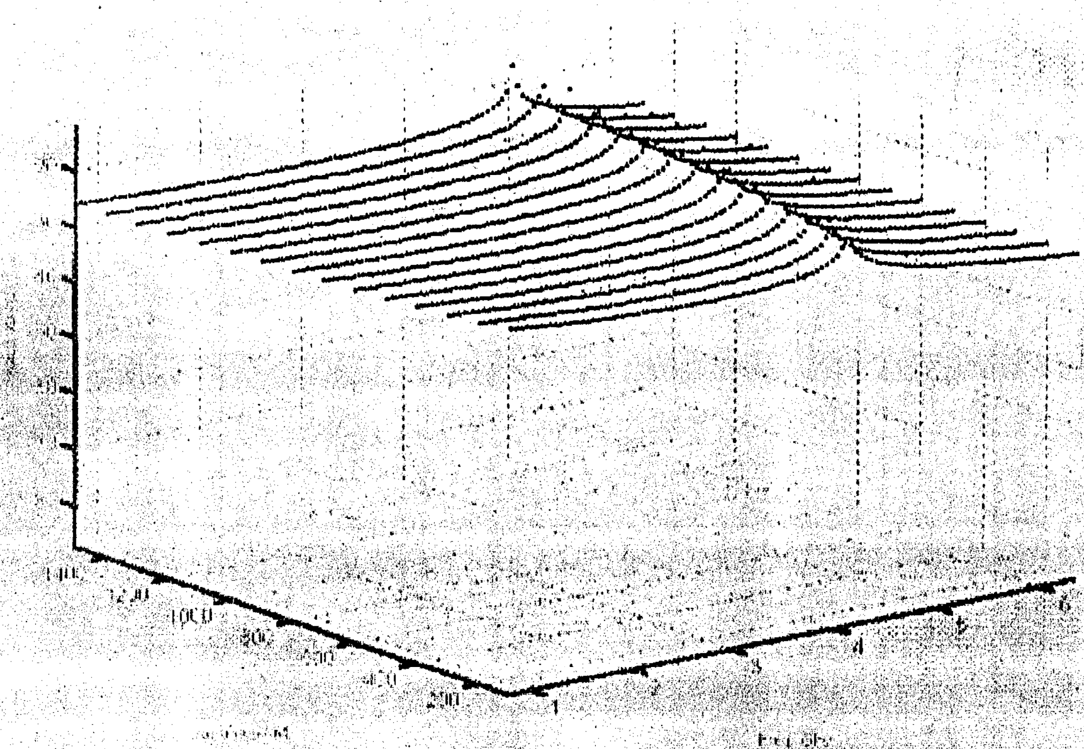

Fig.(8):3-D plot of the noise spectra (RIN 'bold' and FNS 'faint') as a function of feedback rate and frequency. All other parameters were as above.

12

V. CONCLUSION

Noise properties of semiconductor laser operating with phase-conjugate feedback have been studied theoretically using a single mode rate equations modified to cope with this kind of feedback. Noise spectra were calculated, with a main concern on the relative intensity noise and frequency noise spectra. These main noises can tolerate the modulation bandwidth of the laser. A strong resonance formation had been observed in the output of the semiconductor laser. The resonance peak was identified as a result of the interaction between the optical field and the excess carriers in the laser cavity due to phase-conjugate feedback. The height of the relaxation oscillation resonance peak with PCF was very sensitive to the external cavity parameters, namely; time delay, response time, and pumping. For ($\varepsilon = 0$), i.e., for linear gain, the RO resonance peak was washed out. RIN and FNS were found to be drastically dependent on λ_{PCM} for the resonance peak and the noise level. RIN and FNS spectra approached a zero value when $\omega \to 0$, and it was interpreted as phase compensation by the PCM.

APPENDIX A

The Coefficients

Let first write the Laplace transform of the rate equation as:

$$(sI - A - C)\tilde{\chi}(s) = \chi(0) \tag{A1}$$

where A is the part with $\varepsilon=0$. The matrix C represents the contribution of noise and nonlinear gain. From this we derive the inverse transform matrix $sI - A - C$ for noninstantaneous PCF as:

$$A = \begin{pmatrix} a11 & a12 & a13 & -a11 & a12 \\ a21 & a11 & a23 & a21 & a11 \\ a31 & 0 & a33 & 0 & 0 \\ -a11e^{-s\tau} & 0 & 0 & a44 & 0 \\ 0 & -a44e^{-s\tau} & 0 & 0 & a44 \end{pmatrix} \tag{A2}$$

and

$$C = \begin{pmatrix} c11 & 0 & c13 & 0 & 0 \\ 0 & 0 & 0 & 0 & 0 \\ c31 & 0 & c33 & 0 & 0 \\ 0 & 0 & 0 & 0 & 0 \\ 0 & 0 & 0 & 0 & 0 \end{pmatrix} \tag{A3}$$

For instantaneous PCF, the matrices A and C are given by:

$$A = \begin{pmatrix} a11(1-e^{-s\tau}) & a12(1+e^{-s\tau}) & a13 \\ a21(1-e^{-s\tau}) & a11(1-e^{-s\tau}) & a23 \\ a31 & 0 & a33 \end{pmatrix} \tag{A4}$$

and

$$C = \begin{pmatrix} c11 & 0 & c13 \\ 0 & 0 & 0 \\ c31 & 0 & c33 \end{pmatrix} \tag{A5}$$

The coefficients a_{ij} and c_{ij} are given by:

$$a_{11} = -\gamma_{NM}\cos(\beta_s) \tag{A6}$$

$$a_{21} = \frac{\gamma_{NM}}{2P_s}\sin(\beta_s) \tag{A7}$$

$$a_{s} = \left[\frac{1}{\tau_p} + g(N_s - N_0)\right] \tag{A8}$$

$$a_{13} = -2\gamma_{NM}P_s\sin(\beta_s) \tag{A9}$$

14

$$a_{21} = G \cdot P_s \tag{A10}$$

$$a_{22} = \frac{1}{2}\alpha . G_N \tag{A11}$$

$$a = -\left(\frac{1}{\tau_{sp}} + G_N P_s\right) \tag{A12}$$

$$a_{14} = -\frac{1}{t_m} \tag{A13}$$

$$c_1 = -\frac{4\beta N_s}{P_s} \quad \varepsilon . P_s \frac{G_N (N_s - N_{th})(1 - \varepsilon . P_s)}{1 + \varepsilon . P_s} \tag{A14}$$

$$c_{31} = \varepsilon . P_s \frac{(2 + \varepsilon . P_s)\left[\frac{1}{\tau_p} + G_N (N_s - N_{th})\right]}{(1 + \varepsilon . P_s)^2} \tag{A15}$$

$$c_1 = 4\beta \quad \varepsilon . P_s \frac{\varepsilon . P_s}{1 + \varepsilon . P_s} \tag{A16}$$

$$c_{33} = \varepsilon . P_s \frac{\varepsilon P}{1 + \varepsilon . P_s} \tag{A17}$$

The system determinant $D(s) = \det(s.I - A - C)$ can be written as:

$$\begin{aligned} D(s) = {} & s^5 + d_4 s^4 + d_3 s^3 + \left[d_{2c} + d_{21} \exp(-s.\tau)\right] s^2 \\ & + \left[d_{1c} + d_1 \exp(-s.\tau) + d_1 \exp(-2s.\tau)\right] s \\ & \left[d_{0m} + d_0 \exp(-s.\tau) + d_{01} \exp(-2s.\tau)\right] \end{aligned} \tag{A18}$$

where the coefficients d_x are given by:

$$d_4 = -\Gamma_{11} \quad C'' + \frac{2}{t_m} \tag{A19}$$

$$d_3 = -\Gamma_{11}\Gamma_{33} + \Gamma_{13} \tag{A20}$$

$$d_{1c} = \frac{1}{t_m}\left[\Gamma_{11}\Gamma_{33}(2 + A t_m) - \Gamma_{13}(B t_m \quad 2C'' \frac{1}{t_m}) \quad 2B + \frac{C}{t_m}\right] \tag{A21}$$

$$d_{01} = \frac{D}{t_m} \tag{A22}$$

$$d_{0m} = \frac{1}{t_m}\left[\Gamma_{11}\Gamma_{33}(1 + 2A t_m) \quad \Gamma_{13}(2B t_m - 2C'')\right] \tag{A23}$$

15

$$d_{11} = -\frac{1}{t_m}\left(\Gamma_{13}\Gamma_{31}A' + \Gamma_{33}D - \frac{D}{t_m}\right) \quad \text{(A24)}$$

$$d_{12} = -\frac{\gamma_{a\,sp}^{2}}{t_m^{2}} \quad \text{(A25)}$$

$$d_{m} = -\frac{1}{t_m}(\Gamma_{11}\Gamma_{11}A' + \Gamma_{13}B) \quad \text{(A26)}$$

$$d_{14} = -\frac{1}{t_m}[\Gamma_{13}\Gamma_{31}A' + \Gamma_{13}D] \quad \text{(A27)}$$

$$d_{n} = \frac{\Gamma_{11}\gamma_{a\,sp}^{2}}{t_m^{2}} \quad \text{(A28)}$$

We have introduced the parameters below as:

$$\Gamma_{13} = a_{13} + c_{13} \quad \text{(A29)}$$

$$\Gamma_{31} = a_{31} + c_{31} \quad \text{(A30)}$$

$$\Gamma_{33} = a_{33} + c_{33} \quad \text{(A31)}$$

$$\Gamma_{11}A' = a_{31}a_{22} - a_{11}\Gamma_{33} \quad \text{(A32)}$$

$$B = a_{11}c_{31} + \gamma_{a\,sp}^{2} \quad \text{(A33)}$$

$$C = 2a_{1} - c_{1} \quad \text{(A34)}$$

$$D = a_{1}c_{11} \quad \text{(A35)}$$

APPENDIX B

The Minors

For the calculations of the noise spectra, we need the minors $M_{11}(s), M_{13}(s), M_{31}(s)$, and $M_{33}(s)$. They can be written as:

$$Mij = m_{ij,4}s^{4} + m_{ij,3}s^{3} + [m_{ij,2n} + m_{ij,21}\exp(-s.\tau)]s^{2} + [m_{ij,1n} + m_{ij,11}\exp(-s.\tau)]s + [m_{ij,0n} + m_{ij,01}\exp(-s.\tau)] \quad \text{(A36)}$$

The coefficients are given b:

16

$$m_{1,1} = 1 \qquad \text{(A37)}$$

$$m_{1,3} = -\frac{2}{t_m} - H \qquad \text{(A38)}$$

$$m_{1,2n} = J - \frac{2H}{t_m} - \frac{1}{t_m^2} \qquad \text{(A39)}$$

$$m_{1,21} = \frac{a_1}{t_m} \qquad \text{(A40)}$$

$$m_{1,1n} = \frac{1}{t_m}\left(2J - \frac{H}{t_m}\right) \qquad \text{(A41)}$$

$$m_{1,1} = -\frac{a_1}{t_m}\left(\Gamma_{11} - \frac{1}{t_m}\right) \qquad \text{(A42)}$$

$$m_{1,m} = -\frac{J}{t_m^2} \qquad \text{(A43)}$$

$$m_{1,1} = 0 \qquad \text{(A44)}$$

$$m_{2,1} = -a_{21} \qquad \text{(A45)}$$

$$m_{2,2n} = -\frac{2a_{21}}{t_m} - E \qquad \text{(A46)}$$

$$m_{2,21} = \frac{a_{21}}{t_m} \qquad \text{(A47)}$$

$$m_{2,1n} = -\frac{2E}{t_m} - \frac{a_{21}}{t_m^2} \qquad \text{(A48)}$$

$$m_{2,2} = -a_2\left(\frac{1}{t_m^2} - \frac{\Gamma_{21}}{t_m}\right) \qquad \text{(A49)}$$

$$m_{2,1n} = -\frac{E}{t_m^2} \qquad \text{(A50)}$$

$$m_{2,3n} = \frac{a_{21}\Gamma_{21}}{t_m^2} \qquad \text{(A51)}$$

$$m_{2,4} = 0 \qquad \text{(A52)}$$

$$m_{3,1} = a_{31} \qquad \text{(A53)}$$

$$m_{31,2n} = a_{31}\left(\Gamma_{11} - \frac{2}{t_m}\right) \qquad \text{(A54)}$$

$$m_{41,1} = \frac{a_{31}}{t_m} \qquad \text{(A55)}$$

17

$$m_{21,5} = a_{11}\left(\frac{1}{t_m^2} - \frac{2\Gamma_{33}}{t_m}\right) \quad \text{(A56)}$$

$$m_{31,11} = \frac{a_{31}}{t_m}\left(\Gamma_{33} - \frac{1}{t_m}\right) \quad \text{(A57)}$$

$$m_{21,12} = \frac{J}{t_m^2} \quad \text{(A58)}$$

$$m_{31,31} = \frac{J}{t_m^2} \quad \text{(A59)}$$

$$m_{22,4} = 1 \quad \text{(A60)}$$

$$m_{22,2} = \frac{2}{t_m} - G \quad \text{(A61)}$$

$$m_{22,18} = F - \frac{2G}{t_m} + \frac{1}{t_m^2} \quad \text{(A62)}$$

$$m_{22,1} = \frac{a_{31}}{t_m} \quad \text{(A63)}$$

$$m_{22,3} = \frac{1}{t_m}\left(2F - \frac{G}{2t_m}\right) \quad \text{(A64)}$$

$$m_{33,1} = \frac{1}{t_m}\left(-I + \frac{a_{11}}{t_m}\right) \quad \text{(A65)}$$

$$m_{22,30} = \frac{F}{t_m^2} \quad \text{(A66)}$$

$$m_{22,0} = \frac{I}{t_m^2} \quad \text{(A67)}$$

The following parameters have been used for the above minors:

$$\Gamma_{11} = a_{11} + c_1 \quad \text{(A68)}$$

$$L = a_{31}\Gamma_{11} - a_{11}\Gamma_{33} \quad \text{(A69)}$$

$$F = \Gamma_{11}\Gamma_{33} - \Gamma_{13}\Gamma_{31} \quad \text{(A70)}$$

$$G = \Gamma_{11} + \Gamma_{33} \quad \text{(A71)}$$

$$H = a_{31} - \Gamma_{31} \quad \text{(A72)}$$

$$I = a_{11}\Gamma_{33} \quad \text{(A73)}$$

$$J = a_{11}\Gamma_{13} \quad \text{(A74)}$$

18

TABLE I

LASER PARAMETERS* USED IN THE CALCULATIONS.

Parameter	Symbol	Value	Unit
Differential gain	G_N	$1.19\text{x}10^3$	sec^{-1}
Linewidth enhancement factor	α	3	–
Confinement factor	Γ	0.6	–
Nonlinear gain coefficient	ε	$3.57\text{x}10^{-8}$	–
Carrier lifetime	τ_{sp}	2	sec
Threshold inversion	N_{th}	$7.74\text{x}10^8$	–
Carriers transparency	N_o	$3\text{x}10^8$	–
Injection Carriers	J_{th}	$3.87\text{x}10^{17}$	sec^{-1}
Photon lifetime	τ_p	1.4	psec
External cavity roundtrip time	τ	0.5	psec

*(THESE VALUES ARE TYPICAL FOR SEMICONDUCTOR LASER.)

References:

1- M. Nizette, T. Erneux, A. Gavreilides, and V. Kovanis, **Proc. SPIE 3625, 679 (1999).**

2- Ch. Andreeva. Y. Dancheva, M. Taslakov, A. Markovski, P. Zubov, and S. Cartaleva, **Spect. Lett. 34, 395 (2001).**

3- W.A. van der Graaf, L. Pesquera and D. Lenstra, **IEEE J. Quant. Electron. QE-37,562 (2001).**

4- W.A. van der Graaf and L. Pesquera, **Opt. Lett. 23, 256 (1998).**

5- B. Krauskopf, G.R. Gray and D. Lenstra, **Phys. Rev. E-58, 7190 (1998).**

6- M. Yousfi and D. Lenstra, **IEEE J. Quant. Electron. QE-35, 970 (1999).**

7- O.K. Andersen, A.P.A. Fischer, I.C. Lane, E. Louvergneaux, S. Stolte, and D. Lenstra, **ibid QE-35, 577(1999).**

8- A. Murakami and J. Ohstubo, **ibid QE-34, 1979(1998).**

9- T. Erneux, A. Gavreilides and Sciamanna. **Phys. Rev. A-66, 33809(2002).**

10- F. Capasso, R. Paiella, R. Martini, R. Colombelli, C. Gmachl, T.L. Myers, M.S. Taubman, R.M. Williams, C.G. Bethea, K. Unterrainer, H.Y. Hwang, D.L. Svico, A.Y. Cho, M. Sergent, H.C. Liu, and E.A. Whittaker, **IEEE J. Quant. Electron. QE-38, 511 (2002).**

11- S. Eriksson, "Nonlinear Dynamics Of Optically Injected Semiconductor Lasers", PhD Thesis, University of Helsinki, Finland, **(2002).**

12- T. Erneux, A. Gavreilides, K. Green, and B. Krauskopf, **Phys. Rev. E-63 (2003).**